JOC The Journal of Organic Chemistry

pubs.acs.org/joc Article

Concerted [4 + 2] and Stepwise (2 + 2) Cycloadditions of Tetrafluoroethylene with Butadiene: DFT and DLPNO-UCCSD(T) Explorations

Dennis Svatunek,[‖] Ryan P. Pemberton,[‖] Joel L. Mackey, Peng Liu, and K. N. Houk*

Cite This: J. Org. Chem. 2020, 85, 3858−3864 Read Online

ACCESS | Metrics & More | Article Recommendations | Supporting Information

ABSTRACT: Tetrafluoroethylene and butadiene form the 2 + 2 cycloadduct under kinetic control, but the Diels−Alder cycloadduct is formed under thermodynamic control. Borden and Getty showed that the preference for 2 + 2 cycloaddition is due to the necessity for *syn*-pyramidalization of the two CF_2 groups in the 4 + 2 transition state. We have explored the full potential energy surface for the concerted and stepwise reactions of tetrafluoroethylene and butadiene with density functional theory, DFT (B3LYP and M06-2X), DLPNO-UCCSD(T), and CASSCF-NEVPT2 methods and with the distortion/interaction−activation strain model to explain the energetics of different pathways. The 2 + 2 cycloadduct is formed by an anti-transition state followed by two rotations and a final bond formation transition state. Energetics are compared to the reaction of maleic anhydride and ethylene.

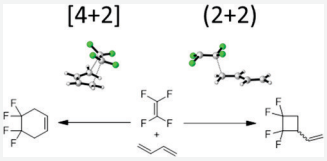

INTRODUCTION

Cycloadditions are versatile synthetic methods to make cyclic molecules through formation of two carbon−carbon or carbon−heteroatom bonds.[1−4] The theoretical rationalizations and predictions of mechanisms of cycloadditions are significant achievements of Woodward and Hoffmann.[5] While dienes and alkenes generally react in a [4 + 2] (Diels−Alder)[6] fashion via a concerted pathway,[7,8] halogenated dienes and alkenes often lead to (2 + 2) adducts by diradical mechanisms.

Bartlett and others found that dienes and halogenated ethylenes often give some, or all, 2 + 2 cycloadducts (Scheme 1).[9−11] Figure 1 shows variable temperature studies performed by Weigert and Davis for the reaction of butadiene (**2**) and tetrafluoroethylene (TFE, **1**).[12] Up to 350 °C, only the 2 + 2 cycloaddition product, 2,2,3,3-tetrafluoro-1-vinylcyclobutane (**3**), was observed. In the range of 350−500 °C, the Diels−Alder product, 4,4,5,5-tetrafluorocyclohexene (**4**), was observed, but double elimination of HF from **4** produced the aromatic product, 1,2-difluorobenzene, above 500 °C.

Scheme 1. (a) Reaction between TFE and Butadiene. (b) Cycloaddition Products of the Reaction of Trifluoroethylene and Butadiene at 215 °C[9]

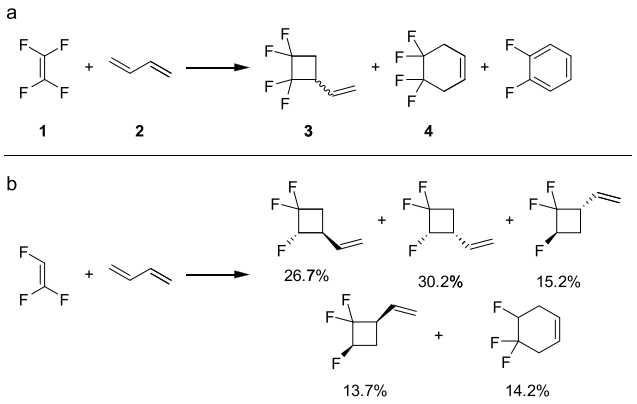

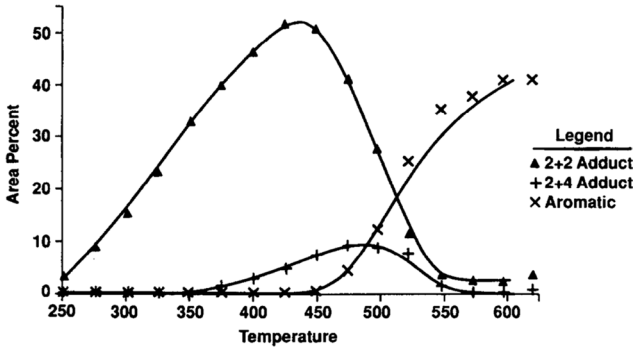

Figure 1. Experimentally determined product distribution of the cycloadducts of **1** and **2** formed as a function of temperature. The temperature is given in °C.[12] Reprinted with the permission of Elsevier.

The reaction of **1** and **2** was studied theoretically by Borden and Wang 30 years ago. They sought to quantify the π-bond strength of TFE.[13] Calculations were performed at the HF/6-31G* level with an MP2 correction to account for electron correlation. It was determined that the origin of the weak π-

Received: January 29, 2020
Published: February 7, 2020

https://dx.doi.org/10.1021/acs.joc.0c00222

bond of **1** was due to the cost of planarizing the two CF_2 groups, highlighting the propensity of fluorine substituents to stabilize the sp^3 geometry (Bent's Rule).[14]

Later, but now 28 years ago, Borden and Getty calculated the energies of diradical intermediates and concluded that the Diels–Alder transition state is energetically unfavorable due to the necessity of *syn*-pyramidalization of the two CF_2 groups.[15]

While the results of Borden explain why the usually favored Diels–Alder reaction is disfavored here, there are many details of these reactions, as well as computational comparisons with systems that favor Diels–Alder additions, that attracted us to this reaction once again. We have studied cycloadditions involving concerted and 2 + 2 diradical pathways using contemporary theoretical methods. The details of mechanisms of 2 + 2 and Diels–Alder reactions and analysis of barriers by the distortion/interaction–activation strain model are reported here. The reactions of TFE were also compared to those of ethene and maleic anhydride.

COMPUTATIONAL METHODS

All stationary points were fully optimized at both UB3LYP/6-311++G(d,p) and UM06-2X/6-311++G(d,p) levels of theory and verified as minima or first-order saddle points with frequency calculations using Gaussian 09.[16] Diradicals were optimized as open-shell singlets. One should be aware of possible shortcomings of density functional theory (DFT) in this regard.[17] Intrinsic reaction coordinate (IRC) calculations were also performed to link transition states to their respective minima. Calculations were performed in the gas phase at 1 atm and 635.15 K. Additionally, DLPNO-UCCSD(T)[18] single-point energy calculations were performed using ORCA 4.0.1[19] and the cc-pVTZ[20] basis set on UB3LYP/6-311++G(d,p) geometries. While UCCSD(T) calculations have been employed in investigations of diradicals,[21] it has been noted that DLPNO-UCCSD(T) can lead to unphysical behavior in case of preceding broken symmetry self-consistent field (SCF) calculations.[22−24] Therefore, the barriers of the rate-determining steps and the electronic nature of intermediate **5** were also investigated using a second-order perturbative treatment of CASSCF wave functions in the form of NEVPT2 calculations as implemented in ORCA. The (2,2) and (4,4) active space was chosen for reactants **1** and **2**, respectively, while (6,6) was used for **TS1**–**TS7** and **5**. Relative energies calculated at the NEVPT2 and DLPNO-UCCSD(T) level are in excellent agreement (Supporting Information, Figure S1). Detailed information about the computational methods is provided in the Supporting Information.

RESULTS AND DISCUSSION

Stationary Points on the Potential Energy Surface. Figure 2 shows the UB3LYP/6-311++G(d,p) optimized geometries of reactants (**1**, **2**) and the products (**3**, **4**) along with the six transition states (**TS1**–**TS6**) that lead to a diradical intermediate and one Diels–Alder transition state (**TS7**) leading to the concerted [4 + 2] product. Diradical formation arises from anti, gauche (+), or gauche (−) conformers about the newly forming C2–C3 bond. Butadiene may be s-*cis* (**2c**) or s-*trans* (**2**). Table 1 shows the computed UB3LYP/6-311++G(d,p), UM06-2X/6-311++G(d,p), and DLPNO-UCCSD(T)/cc-pVTZ single-point calculations, all of which predict that transition state **TS1**, which involves anti-attack on s-*trans* butadiene, has the lowest activation energy.

DLPNO-UCCSD(T) calculations predict that the three approaches involving s-*trans*-butadiene (**TS1**–**TS3**) are approximately 2.5 kcal/mol lower in energy than the corresponding approaches involving s-*cis*-butadiene (**TS4**–**TS6**), since butadiene prefers the s-*trans* conformation by 2.9 kcal/mol. The anti-transition states, **TS1** and **TS4**, are more stable than their gauche (+) and gauche (−) counterparts by 1.6–2.2 kcal/mol.

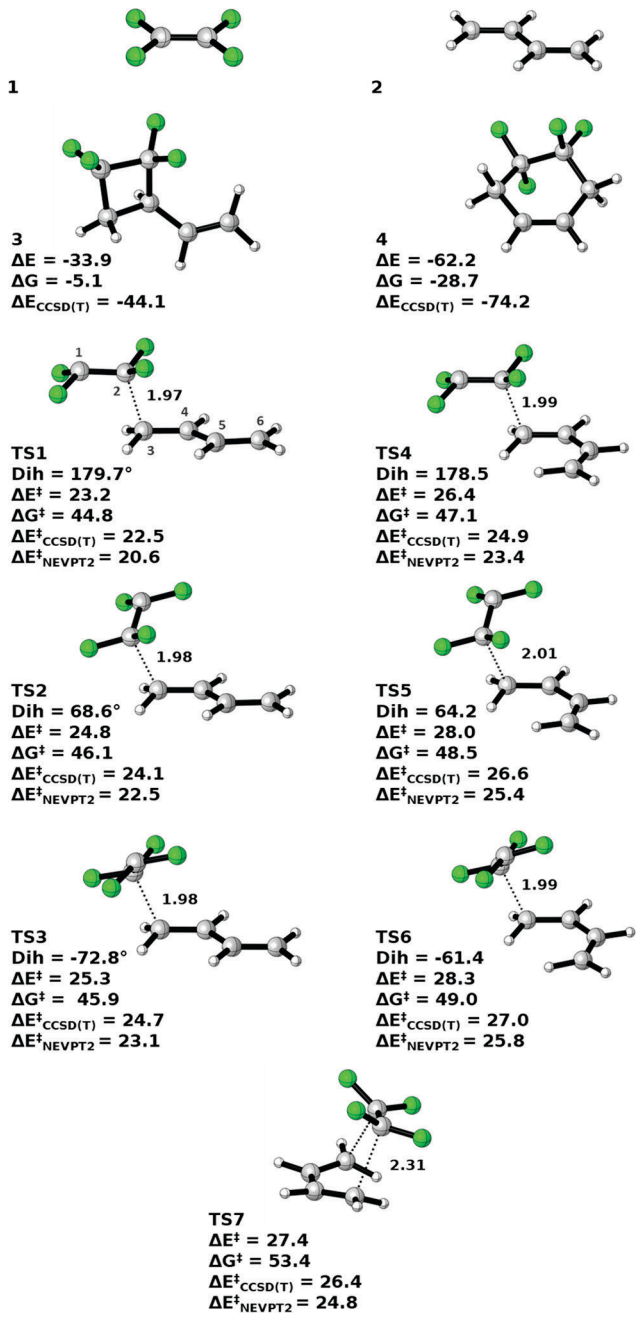

Figure 2. UB3LYP/6-311++G(d,p) optimized geometries and relative ΔE and $\Delta G_{635\,K}$ energies of diradical-forming transition states (**TS1**–**TS6**) and the Diels–Alder transition state, **TS7**. Values shown are the forming bond length (C2–C3, in Å) and dihedral (C1–C2–C3–C4, indicating anti, gauche +, and gauche −) angle about the forming bond. Energies are relative to reactants **1** and **2** and are in kcal/mol. DPLNO-UCCSD(T)/cc-pVTZ//UB3LYP/6-311++G(d,p) and in case of transition states NEVPT2/def2-TZVP//UB3LYP/6-311++G(d,p), single-point electronic energies are also given. Numbering of carbon atoms in TS and intermediates is demonstrated in **TS1**.

At the UB3LYP/6-31++G(d,p) and DLPNO-UCCSD(T)/cc-pVTZ//UB3LYP/6-311++G(d,p) levels of theory, the concerted Diels–Alder transition state, **TS7**, is 3.9–4.2 kcal/

Table 1. Calculated Electronic Energies, Enthalpies, and Free Energies (in kcal/mol) at 623.15 K for 1−8 and TS1−TS12 at the Indicated Level of Theory

	UB3LYP/6-311++G(d,p)			UM06-2X/6-311++G(d,p)			DLPNO-UCCSD(T)/cc-pVTZ//UB3LYP/6-311++G(d,p)
	ΔE	ΔH	ΔG	ΔE	ΔH	ΔG	ΔE
1 + 2	0.0	0.0	0.0	0.0	0.0	0.0	0.0
3	−33.9	−31.2	−5.1	−47.1	−44.3	−17.3	−44.1
4	−62.2	−59.1	−28.7	−77.8	−74.5	−44.0	−74.2
5	10.2	11.8	32.5	5.6	7.1	28.5	13.4
6	10.9	12.4	33.0	5.7	7.2	28.9	11.9
7	9.5	11.0	31.7	4.4	6.0	27.4	10.9
8	11.4	12.9	33.8	6.3	7.8	28.6	12.1
TS1	23.2	23.5	44.8	22.2	22.4	44.3	22.5
TS2	24.8	15.0	46.1	23.6	23.7	45.5	24.2
TS3	25.3	25.4	45.9	24.2	24.1	45.1	24.9
TS4	26.4	26.8	47.1	24.6	24.8	46.4	25.1
TS5	28.0	28.3	48.5	26.1	26.3	47.9	26.9
TS6	28.3	28.6	49.0	26.4	26.5	48.3	27.4
TS7	27.4	28.2	53.4	20.5	21.5	47.7	26.4
TS8	13.7	14.0	38.7	9.3	9.7	35.0	14.7
TS9	13.5	13.7	38.8	8.5	8.6	34.1	15.5
TS10	9.5	11.0	31.7	5.1	5.5	30.6	9.8
TS11	14.3	14.6	39.2	9.9	10.1	35.4	16.6
TS12	16.3	16.5	38.0	11.7	11.8	34.1	23.1

mol higher in energy than the lowest diradical-forming transition state, TS_1, while $\Delta\Delta G^{\ddagger}$ is 8.6 kcal/mol.

IRC calculations reveal that transition structures **TS1**, **TS2**, and **TS3** lead directly to diradical intermediates **5**, **8**, and **6**, respectively (Figure 3). Here, only the s-*trans*-butadiene reactant will be discussed, since the potential energy surface (PES) involving the s-*cis*-butadiene reactant is higher in energy by about 3 kcal/mol. The diradical intermediates **5** and **8** can

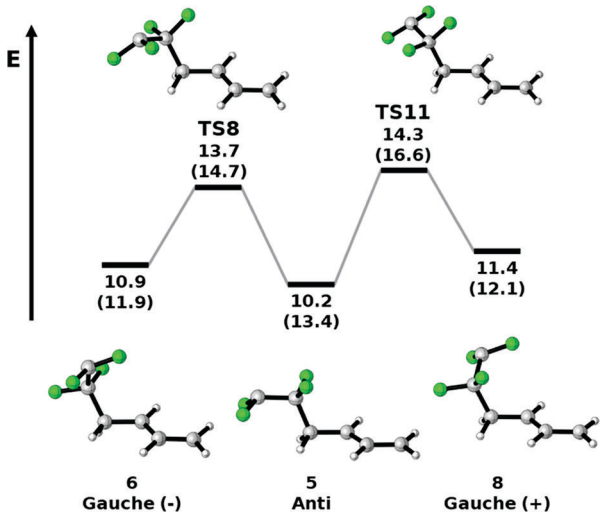

Figure 3. Rotational transition states (**TS8** and **TS11**) linking diradical minima **5**, **6**, and **8** via rotation around the C2-C3 bond. UB3LYP/6-311++G(d,p) electronic energies are shown in plain text and DLPNO-UCCSD(T)/cc-pVTZ//UB3LYP/6-311++G(d,p) single-point energies are in parenthesis. Both sets of energies are given in kcal/mol, relative to the reactants **1** and **2**.

be interconverted to **6** by transition states **TS8** and **TS11** (Figure 3) corresponding to rotation around the C2−C3 bond.

Once intermediate **6** is formed, inversion of the radical center at C1 is necessary to align the two radicals on C1 and C4, making ring closure facile.

This can be accomplished by inversion through a planar high-energy transition state **TS12** or by rotation around the C1−C2 bond through **TS9** (Figure 4). This rotation avoids the unfavorable planarization of the radical on C1. The rotational barrier for the conversion of **6** to **7** is 2.6 kcal/mol.

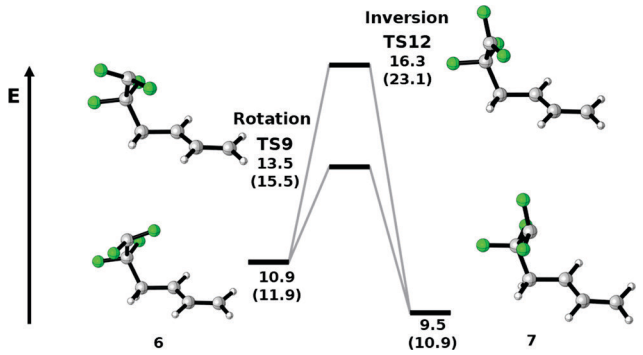

Figure 4. Diradical rotational transition state (**TS9**) and radical inversion (**TS12**) linking local minima **6** to **7**. UB3LYP/6-311++G(d,p) electronic energies are shown in plain text and DLPNO-UCCSD(T)/cc-pVTZ//UB3LYP/6-311++G(d,p) single-point energies are in parenthesis. Both sets of energies are given in kcal/mol relative to the reactants **1** and **2**.

The minimum energy reaction paths (MERPs) for the formation of **3** and the concerted [4 + 2] cycloaddition pathway to form **4** are shown in Figure 5.

The MERP leading to the 2 + 2 adduct includes a flat, entropically controlled energy surface after the initial formation of a diradical. Similar energy surfaces have been described for other diradicals such as the tetramethylene species.[25] The anti-diradical-forming transition state on s-*trans*-butadiene is the rate-limiting step for the formation of **3**. For **5** to form **3**, a vibrational mode corresponding to rotation around the C2−C3 bond must be activated in addition to the inversion of the radical at C1 by rotation through **TS9** or inversion (**TS12**). The ring closure proceeds through a near barrierless reaction step (**TS10**). In accordance with experimental results, the concerted [4 + 2] pathway to form **4** is kinetically disfavored by 4(E) to 6(G) kcal/mol over the diradical pathway forming the (2 + 2) product **3**, but product **4** is thermodynamically favored over **3** by about 30 kcal/mol.

No direct pathway from s-*cis*- or s-*trans*-butadiene derived diradical species to the [4 + 2] product **4** could be found.

Distortion/Interaction−Activation Strain Analysis. The preference for the kinetically controlled formation of **3** can be explained using the distortion/interaction−activation strain analysis,[26−33] which was conducted using autoDIAS.[34] In this analysis, the activation energy, $\Delta E^{\ddagger}$, is divided into two components. The first component, $\Delta E^{\ddagger}_{dist}$, gives the energy required to distort the reactants to their transition state geometries without interactions. The second component, $\Delta E^{\ddagger}_{int}$, is the interaction energy between distorted reactants, usually a stabilizing effect. The sum of $\Delta E^{\ddagger}_{dist}$ and $\Delta E^{\ddagger}_{int}$ equals the energy of activation, $\Delta E^{\ddagger}$. This analysis has been successfully applied to explain the reactivity in various

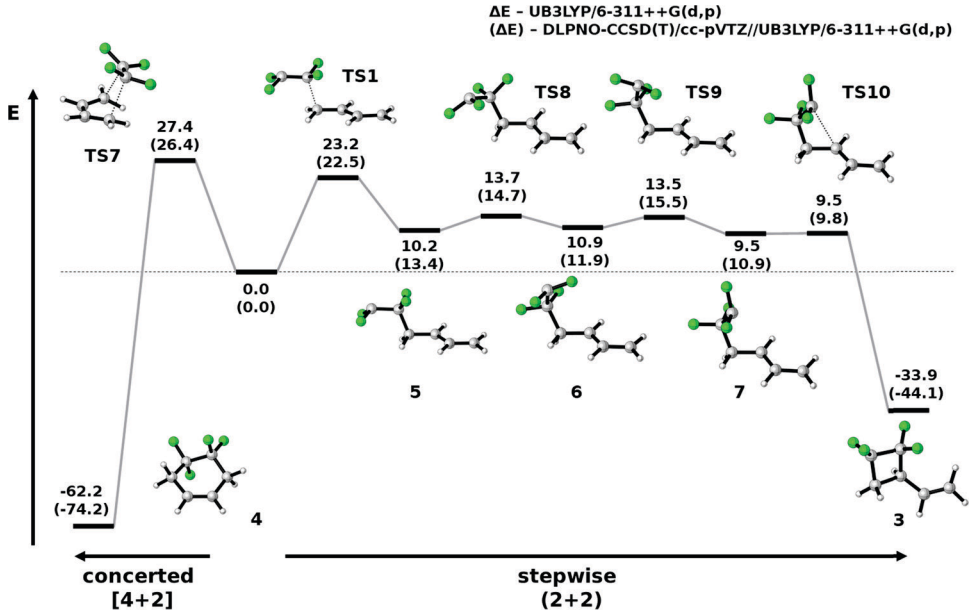

Figure 5. Minimum energy reaction pathways for formation of **3** and **4**.

cycloaddition reactions.[35−44] We compared the reactions of butadiene with ethylene **9** and maleic anhydride **10**, which both yield exclusively Diels−Alder adducts, and butadiene with tetrafluoroethylene **1**, which gives the 2 + 2 adduct through diradical **5**. UB3LYP/6-311++G(d,p) structures were used for the distortion/interaction−activation strain analysis shown in Figure 6. The high distortion energy of the dienophile TFE (18.2 kcal/mol) in the Diels−Alder transition state **TS7** provides an explanation for the high energy of the concerted pathway in contrast to similar 4 + 2 cycloadditions. In the two prototypical Diels−Alder reactions with dienophiles **9** and **10**, the dienophile distortion energy is much lower (8.6 and 10.2 kcal/mol, respectively). The high dienophile distortion energy in **TS7** is attributed to *syn*-pyramidalization, which distorts the relatively negative fluorine substituents into proximity. This is Getty and Borden's conclusion.[15]

By contrast, the stepwise 2 + 2 cycloaddition with tetrafluoroethylene has a low diene distortion energy (6.3 kcal/mol) in **TS1**, thus leading to an overall decreased energy of activation and preference for this pathway. The distortion energy of tetrafluoroethylene in the diradical pathway, 17.9 kcal/mol, is similar to the value found for the concerted [4 + 2] cycloaddition (18.2 kcal/mol). This can be explained by the fact that in **TS7**, the out of plane bending of the fluorides in TFE is only 15° and the forming bond distance is 2.30 Å while in **TS1**, the bending is much stronger with 22° and the forming bond distance is shorter with 1.97 Å. However, in **TS1**, the second CF_2 unit is free to adopt any conformation, which allows for better stabilization through anti-pyramidalization, while in **TS7**, unfavorable *syn*-pyramidalization is enforced leading to similar distortion energy at lower geometric distortion. Figure 7 shows the TFE distortion energies along intrinsic reaction coordinates calculated for the [4 + 2] cycloaddition proceeding through **TS7** and the diradical-forming reaction going through **TS1**. As shown, for a given angle, the distortion energy is higher in the case of the [2 + 4] reaction due to the forced *syn*-pyramidalization. The preference of alkenes and alkynes for *anti*-pyramidalization in both radical and ionic cases is well established.[13,45−47]

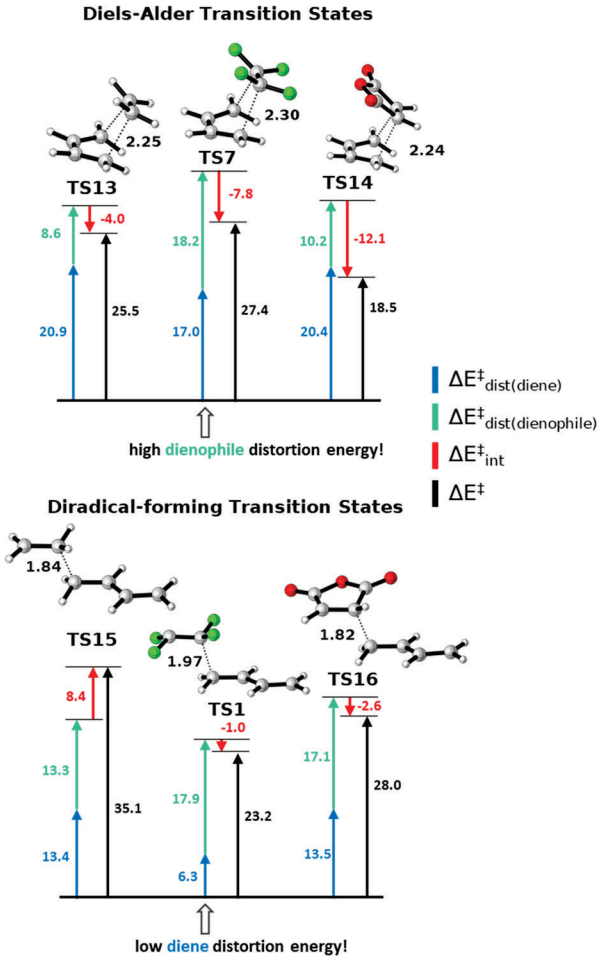

Figure 6. Distortion/interaction−activation strain analysis at the UB3LYP/6-311++G(d,p) level of theory. All values are in kcal/mol.

Compared to the 2 + 2 diradical pathways of ethylene (**9**) and maleic anhydride (**10**), the forming C2−C3 bond length in **TS1** is significantly longer than those in **TS15** and **TS16**.

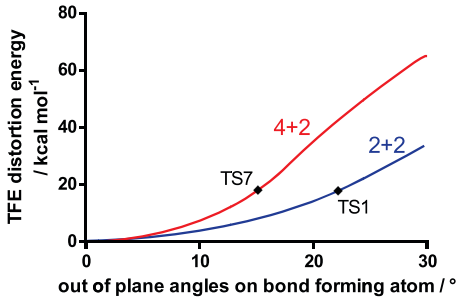

Figure 7. Distortion energies of TFE along the reaction coordinate defined by the out of plane angle on bond-forming centers. Positions of **TS1** and **TS7** are indicated.

Thus, the diene in **TS1** does not need to distort much to achieve the transition structure geometry resulting in the low diene distortion energy of only 6.3 kcal/mol. The earlier **TS1** can be attributed to the better stabilization of the forming diradical. The Diels–Alder transition state with maleic anhydride (**TS14**) is stabilized largely by the interaction energy (-12.1 kcal/mol), while maleic anhydride fails to stabilize the radical center formed in **TS16**, leading to a later transition state. In **TS15**, a positive (energetically destabilizing) interaction energy of 8.4 kcal/mol is observed due to the inability of hydrogen to stabilize radicals, making the 2 + 2 pathway not feasible.

Energy of Concert. The energy by which the activation energy of the concerted reaction is favored over stepwise reaction is the energy of concert.[48] Figure 8 shows energy of concert analyses for the three reactions described earlier. The reaction of **2** with **1** has negative energy of concert. The stepwise reaction is preferred in this case by 4.2 kcal/mol. Reactions of **2** with **9** or **10** have positive energies of concert. The concerted mechanism is favored with similar energy of concert values, 9.6 and 9.5 kcal/mol, respectively. Previous calculations for butadiene and ethylene predicted energies of concert of 2–7 kcal/mol.[49]

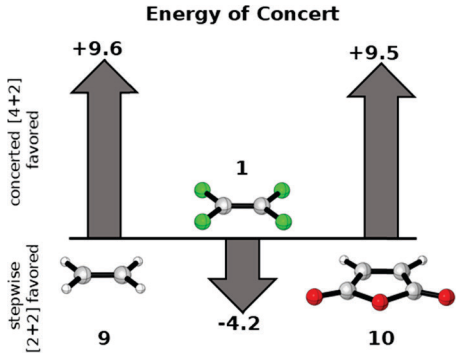

Figure 8. Energies of concert for alkenes **9**, **1**, and **10**. All values are in kcal/mol.

The stepwise reaction is preferred in the TFE case because the diradical intermediates and the transition states leading to them are stabilized. By contrast, the maleic anhydride dienophile stabilizes the concerted pathway to a large extent and the stepwise pathway less, although it does stabilize that also. The interaction energy in **TS14** plays a large role in the stabilization of the [4 + 2] cycloaddition pathway for maleic anhydride; this arises from the well-known charge transfer interactions resulting from the small highest occupied molecular orbital–lowest unoccupied molecular orbital (HOMO–LUMO) gap. The absence of energetically unfavorable *syn*-pyramidalization of CF_2 centers in the dienophile of **TS13** versus **TS7** lowers the electronic energy of this transition state.

CONCLUSIONS

The stepwise (2 + 2) cycloaddition is kinetically preferred over the concerted Diels–Alder reaction for the butadiene–TFE reaction. The *syn*-pyramidalization penalty identified by Borden and Getty for the concerted reaction is consistent with this model. In addition, we identified the low diene distortion in the stepwise (2 + 2) cycloaddition as an important factor for the preference of this pathway.

Diradical transition structures **TS1**–**TS6** are all lower in energy than the Diels–Alder transition state, **TS7**. These six transition states can all form the (2 + 2) cycloaddition product. The MERP in Figure 5 shows that a preference for antidiradical formation dominates, and subsequent rotation around the C2–C3 bond followed by radical inversion along a flat PES eventually affords the kinetic (2 + 2) cycloaddition product.

ASSOCIATED CONTENT

Supporting Information

The Supporting Information is available free of charge at https://pubs.acs.org/doi/10.1021/acs.joc.0c00222.

UB3LYP and UM06-2X optimized geometries for all structures and detailed information on the computational methods; energies of UB3LYP/6-311++G(d,p) and UM06-2X/6-311++G(d,p) calculated structures; correlation between UCCSD(T) and NEVPT2 calculated relative energies; UCCSD(T) and NEVPT2 calculated energies (PDF)

AUTHOR INFORMATION

Corresponding Author

K. N. Houk – *Department of Chemistry and Biochemistry, University of California, Los Angeles, California 90095, United States;* orcid.org/0000-0002-8387-5261; Email: houk@chem.ucla.edu

Authors

Dennis Svatunek – *Department of Chemistry and Biochemistry, University of California, Los Angeles, California 90095, United States;* orcid.org/0000-0003-1101-2376

Ryan P. Pemberton – *Department of Chemistry, University of California, Davis, California 95616, United States*

Joel L. Mackey – *Department of Chemistry and Biochemistry, University of California, Los Angeles, California 90095, United States*

Peng Liu – *Department of Chemistry, University of Pittsburgh, Pittsburgh, Pennsylvania 15260, United States;* orcid.org/0000-0002-8188-632X

Complete contact information is available at: https://pubs.acs.org/10.1021/acs.joc.0c00222

Author Contributions

‖D.S. and R.P.P. contributed equally.

Notes

The authors declare no competing financial interest.

■ ACKNOWLEDGMENTS

The authors are grateful to the National Science Foundation (CHE-1764328) for financial support of this research. Computations were performed using the Extreme Science and Engineering Discovery Environment (XSEDE), which is supported by the National Science Foundation grant number ACI-1548562 and by the UCLA Institute for Digital Research and Education (IDRE). D.S. is grateful to the Austrian Science Funds (FWF, J4216-N28).

■ REFERENCES

(1) Huisgen, R. Cycloadditions - Definition, Classification, and Characterization. *Angew. Chem., Int. Ed.* **1968**, *7*, 321−406.
(2) Potts, K. In *1,3-Dipolar Cycloaddition Chemistry*; Padwa, A., Ed.; Wiley-Interscience: New York, NY, 1984.
(3) Nicolaou, K. C.; Snyder, S. A.; Montagnon, T.; Vassilikogiannakis, G. The Diels−Alder reaction in total synthesis. *Angew. Chem., Int. Ed.* **2002**, *41*, 1668−1698.
(4) Ylijoki, K. E.; Stryker, J. M. [5 + 2] Cycloaddition reactions in organic and natural product synthesis. *Chem. Rev.* **2012**, *113*, 2244−2266.
(5) Woodward, R. B.; Hoffmann, R. The conservation of orbital symmetry. *Angew. Chem., Int. Ed.* **1969**, *8*, 781−853.
(6) Diels, O.; Alder, K. Synthesen in der hydroaromatischen Reihe. *Justus Liebigs Ann. Chem.* **1928**, *460*, 98−122.
(7) Houk, K.; Lin, Y. T.; Brown, F. K. Evidence for the concerted mechanism of the Diels-Alder reaction of butadiene with ethylene. *J. Am. Chem. Soc.* **1986**, *108*, 554−556.
(8) Black, K.; Liu, P.; Xu, L.; Doubleday, C.; Houk, K. N. Dynamics, transition states, and timing of bond formation in Diels−Alder reactions. *Proc. Natl. Acad. Sci. U.S.A.* **2012**, *109*, 12860−12865.
(9) Bartlett, P. D. 1,2- and 1,4-Cycloaddition to Conjugated Dienes. *Science* **1968**, *159*, 833−838.
(10) Coffman, D. D.; Barrick, P. L.; Cramer, R. D.; Raasch, M. S. Synthesis of Tetrafluorocyclobutanes by Cycloalkylation. *J. Am. Chem. Soc.* **1949**, *71*, 490−496.
(11) Bartlett, P. D.; Schueller, K. E. Cycloaddition. VIII. Ethylene as a dienophile. A minute amount of 1,2-cycloaddition of ethylene to butadiene. *J. Am. Chem. Soc.* **1968**, *90*, 6071−6077.
(12) Weigert, F. J.; Davis, R. F. Synthesis and aromatization of 2 + 2 cycloadducts of butadienes and tetrafluoroethylene. *J. Fluorine Chem.* **1993**, *63*, 69−84.
(13) Wang, S. Y.; Borden, W. T. Why is the.pi. bond in tetrafluoroethylene weaker than that in ethylene? An ab initio investigation. *J. Am. Chem. Soc.* **1989**, *111*, 7282−7283.
(14) Bent, H. A. An Appraisal of Valence-bond Structures and Hybridization in Compounds of the First-row elements. *Chem. Rev.* **1961**, *61*, 275−311.
(15) Getty, S. J.; Borden, W. T. Why does tetrafluoroethylene not undergo Diels-Alder reaction with 1,3-butadiene? An ab initio investigation. *J. Am. Chem. Soc.* **1991**, *113*, 4334−4335.
(16) Frisch, M.; Trucks, G.; Schlegel, H.; Scuseria, G.; Robb, M.; Cheeseman, J.; Scalmani, G.; Barone, V.; Mennucci, B.; Petersson, G. *Gaussian 09*, revision D.01; Gaussian Inc.: Wallingford, CT, 2009.
(17) Gräfenstein, J.; Kraka, E.; Filatov, M.; Cremer, D. Can Unrestricted Density-Functional Theory Describe Open Shell Singlet Biradicals? *Int. J. Mol. Sci.* **2002**, *3*, 360−394.
(18) Riplinger, C.; Sandhoefer, B.; Hansen, A.; Neese, F. Natural triple excitations in local coupled cluster calculations with pair natural orbitals. *J. Chem. Phys.* **2013**, *139*, No. 134101.
(19) Neese, F. Software update: the ORCA program system, version 4.0. *Wiley Interdiscip. Rev.: Comput. Mol. Sci.* **2018**, *8*, No. e1327.
(20) Dunning, T. H. Gaussian basis sets for use in correlated molecular calculations. I. The atoms boron through neon and hydrogen. *J. Chem. Phys.* **1989**, *90*, 1007−1023.
(21) Tentscher, P. R.; Arey, J. S. Geometries and Vibrational Frequencies of Small Radicals: Performance of Coupled Cluster and More Approximate Methods. *J. Chem. Theory Comput.* **2012**, *8*, 2165−2179.
(22) Piecuch, P.; Kowalski, K.; Pimienta, I. S. O.; McGuire, M. J. Recent advances in electronic structure theory: Method of moments of coupled-cluster equations and renormalized coupled-cluster approaches. *Int. Rev. Phys. Chem.* **2002**, *21*, 527−655.
(23) Crawford, T. D.; Schaefer, H. F. An Introduction to Coupled Cluster Theory for Computational Chemists. In *Reviews in Computational Chemistry*; Wiley, 2007; pp 33−136.
(24) ORCA 4.0.1 Manual. https://cec.mpg.de/fileadmin/media/Forschung/ORCA/orca_manual_4_0_1.pdf.
(25) Doubleday, C. Tetramethylene. *J. Am. Chem. Soc.* **1993**, *115*, 11968−11983.
(26) Lam, Y.-h.; Cheong, P. H.-Y.; Mata, J. M. B.; Stanway, S. J.; Gouverneur, V.; Houk, K. N. Diels-Alder Exo Selectivity in Terminal-Substituted Dienes and Dienophiles: Experimental Discoveries and Computational Explanations. *J. Am. Chem. Soc.* **2009**, *131*, 1947−1957.
(27) Bickelhaupt, F. M.; Houk, K. N. Analyzing Reaction Rates with the Distortion/Interaction-Activation Strain Model. *Angew. Chem., Int. Ed.* **2017**, *56*, 10070−10086.
(28) Bickelhaupt, F. M. Understanding reactivity with Kohn-Sham molecular orbital theory: E2-SN2 mechanistic spectrum and other concepts. *J. Comput. Chem.* **1999**, *20*, 114−128.
(29) te Velde, G.; Bickelhaupt, F. M.; Baerends, E. J.; Guerra, C. F.; van Gisbergen, S. J. A.; Snijders, J. G.; Ziegler, T. Chemistry with ADF. *J. Comput. Chem.* **2001**, *22*, 931−967.
(30) Diefenbach, A.; Bickelhaupt, F. M. Oxidative addition of Pd to C−H, C−C and C−Cl bonds: Importance of relativistic effects in DFT calculations. *J. Chem. Phys.* **2001**, *115*, 4030−4040.
(31) Diefenbach, A.; Bickelhaupt, F. M. Activation of C−H, C−C and C−I bonds by Pd and cis-$Pd(CO)_2I_2$. Catalyst−substrate adaptation. *J. Organomet. Chem.* **2005**, *690*, 2191−2199.
(32) van Stralen, J. N. P.; Bickelhaupt, F. M. Oxidative Addition versus Dehydrogenation of Methane, Silane, and Heavier AH_4 Congeners Reacting with Palladium. *Organometallics* **2006**, *25*, 4260−4268.
(33) de Jong, G. T.; Visser, R.; Bickelhaupt, F. M. Oxidative addition to main group versus transition metals: Insights from the Activation Strain model. *J. Organomet. Chem.* **2006**, *691*, 4341−4349.
(34) Svatunek, D.; Houk, K. N. autoDIAS: a python tool for an automated distortion/interaction activation strain analysis. *J. Comput. Chem.* **2019**, *40*, 2509−2515.
(35) Svatunek, D.; Houszka, N.; Hamlin, T. A.; Bickelhaupt, F. M.; Mikula, H. Chemoselectivity of Tertiary Azides in Strain-Promoted Alkyne-Azide Cycloadditions. *Chem. − Eur. J.* **2019**, *25*, 754−758.
(36) Riesco-Domínguez, A.; van de Wiel, J.; Hamlin, T. A.; van Beek, B.; Lindell, S. D.; Blanco-Ania, D.; Bickelhaupt, F. M.; Rutjes, F. P. J. T. Trifluoromethyl Vinyl Sulfide: A Building Block for the Synthesis of CF_3S-Containing Isoxazolidines. *J. Org. Chem.* **2018**, *83*, 1779−1789.
(37) Gold, B.; Aronoff, M. R.; Raines, R. T. 1,3-Dipolar Cycloaddition with Diazo Groups: Noncovalent Interactions Overwhelm Strain. *Org. Lett.* **2016**, *18*, 4466−4469.
(38) Escorihuela, J.; Das, A.; Looijen, W. J. E.; van Delft, F. L.; Aquino, A. J. A.; Lischka, H.; Zuilhof, H. Kinetics of the Strain-Promoted Oxidation-Controlled Cycloalkyne-1,2-quinone Cycloaddition: Experimental and Theoretical Studies. *J. Org. Chem.* **2018**, *83*, 244−252.
(39) Cabrera-Trujillo, J. J.; Fernández, I. Understanding exo-selective Diels−Alder reactions involving Fischer-type carbene complexes. *Org. Biomol. Chem.* **2019**, *17*, 2985−2991.
(40) Fernández, I. Understanding the Reactivity of Fullerenes Through the Activation Strain Model. *Eur. J. Org. Chem.* **2018**, *2018*, 1394−1402.
(41) García-Rodeja, Y.; Fernández, I. Factors Controlling the Reactivity of Strained-Alkyne Embedded Cycloparaphenylenes. *J. Org. Chem.* **2019**, *84*, 4330−4337.

(42) Wang, Z.; Danovich, D.; Ramanan, R.; Shaik, S. Oriented-External Electric Fields Create Absolute Enantioselectivity in Diels–Alder Reactions: Importance of the Molecular Dipole Moment. *J. Am. Chem. Soc.* **2018**, *140*, 13350–13359.
(43) Gomes, G. d. P.; Loginova, Y.; Vatsadze, S. Z.; Alabugin, I. V. Isonitriles as Stereoelectronic Chameleons: The Donor–Acceptor Dichotomy in Radical Additions. *J. Am. Chem. Soc.* **2018**, *140*, 14272–14288.
(44) Schoenebeck, F.; Ess, D. H.; Jones, G. O.; Houk, K. N. Reactivity and Regioselectivity in 1,3-Dipolar Cycloadditions of Azides to Strained Alkynes and Alkenes: A Computational Study. *J. Am. Chem. Soc.* **2009**, *131*, 8121–8133.
(45) Volland, W. V.; Davidson, E. R.; Borden, W. T. Effect of carbon atom pyramidalization on the bonding in ethylene. *J. Am. Chem. Soc.* **1979**, *101*, 533–537.
(46) Borden, W. T. Pyramidalized alkenes. *Chem. Rev.* **1989**, *89*, 1095–1109.
(47) Strozier, R. W.; Caramella, P.; Houk, K. N. Influence of molecular distortions upon reactivity and stereochemistry in nucleophilic additions to acetylenes. *J. Am. Chem. Soc.* **1979**, *101*, 1340–1343.
(48) Mirand, C.; Massiot, G.; Levy, J. A synthetic entry in the Aristotelia alkaloids. *J. Org. Chem.* **1982**, *47*, 4169–4170.
(49) Goldstein, E.; Beno, B.; Houk, K. N. Density Functional Theory Prediction of the Relative Energies and Isotope Effects for the Concerted and Stepwise Mechanisms of the Diels–Alder Reaction of Butadiene and Ethylene. *J. Am. Chem. Soc.* **1996**, *118*, 6036–6043.

https://dx.doi.org/10.1021/acs.joc.9b03233